NATIONAL ADVISORY COMMITTEE FOR AERONAUTICS

TECHNICAL NOTE 3091

FLOW PROPERTIES OF STRONG SHOCK WAVES IN XENON GAS AS DETERMINED FOR THERMAL EQUILIBRIUM CONDITIONS

By Alexander P. Sabol

Langley Aeronautical Laboratory
Langley Field, Va.

NACA

Washington
December 1953

E

NATIONAL ADVISORY COMMITTEE FOR AERONAUTICS

TECHNICAL NOTE 3091

FLOW PROPERTIES OF STRONG SHOCK WAVES IN XENON GAS AS DETERMINED FOR THERMAL EQUILIBRIUM CONDITIONS

By Alexander P. Sabol

SUMMARY

The results of calculations are presented for the purpose of showing the effects of ionization and electronic excitation on the flow properties of one-dimensional shock waves in xenon gas. The calculations are based on statistical-mechanics theory with the assumption that thermal equilibrium exists at all points in the flow. The calculations are made by both including and neglecting the effects of electronic excitation, and the results of the calculations are qualitatively compared with experimental data.

INTRODUCTION

Air in passing through sufficiently strong shock waves does not behave as an ideal fluid because of the effects resulting from molecular dissociation, electronic excitation, and ionization. Several theoretical investigations of such strong shocks have been made by using the methods of statistical mechanics (refs. 1 and 2). The experimental investigations of strong shocks in air have been hindered by the difficulty in producing them. However, in an effort to study these effects, strong shock waves have been produced in other gases (refs. 3 to 5).

Resler, Lin, and Kantrowitz (ref. 4) examined the flow of argon in shock tubes and obtained both experimental and theoretical results. This investigation indicated that no flow effects would be attributed to electronic excitation for flow velocities up to a Mach number normal to the shock of 20; therefore, the theoretical calculations were simplified by neglecting electronic excitation. The work of reference 3 consisted of an investigation, by a ballistic method, of strong shock flows about small metal cone-cylinder models in xenon, in which higher Mach number flows can be obtained than in argon.

The purpose of this paper is to present the results of theoretical calculations of the flow properties of xenon in strong shock waves.

Two sets of calculations are made, one including the effects of electronic excitation and ionization, designated as excitation calculations, and the other including only the effects of ionization, designated as nonexcitation calculations. The excitation calculations follow the method described in reference 1. The results of the calculations are qualitatively compared with experimental results given in reference 3 on the assumption that the glow observed in a xenon shock wave is approximately proportional to the percent ionization.

SYMBOLS

γ	adiabatic index, 5/3
Xe	xenon $\left(\text{atomic weight, } 131.3 \frac{\text{g}}{\text{mole}}\right)$
N_o	Avogadro's number, $6.02544 \times 10^{23} \frac{\text{molecules}}{\text{mole}}$
k	Boltzmann's constant, $1.38026 \times 10^{-16} \frac{\text{ergs}}{^{\circ}\text{K-molecule}}$
m_e	electron mass, 9.10721×10^{-28}, g
E	energy, ergs/mole
σ	energy equivalent, $1.60186 \times 10^{-12} \frac{\text{ergs}}{\text{electron volt}}$
K	equilibrium constant
χ	first ionization potential of xenon, 12.078 electron volts
α	ionization, percent
M	free-stream Mach number
M_1	Mach number normal to shock, $\frac{u_1}{\sqrt{\gamma p_1 v_1}}$
m	mass
δ	one-half included angle of cone, deg

Z	partition function
h	Planck's constant, 6.62377×10^{-27} erg-sec
p	pressure, dynes/cm^2
u_c/u_l	ratio of velocity on cone surface to limiting velocity
θ	shock-wave angle, deg
V	volume, $\frac{cm^3}{g\text{-mole}}$
g_n	statistical weight
T	temperature, ^oK
$\tilde{\nu}_n$	term-value difference, cm^{-1}
J	total angular momentum of molecule
R	universal gas constant, $N_o k$, $\frac{ergs}{^oK\text{-mole}}$
u	velocity, cm/sec
c	velocity of light, 2.99790×10^{10} cm/sec

Subscripts:

I	non-ionized or neutral atom
II	ionized atom
1	a point in the otherwise undisturbed stream
2	a point immediately behind shock wave
e	electron
ex	atomic excitation
i	internal part
ion	atomic ionization

n the nth term

t atomic translation, also translational part

The term mole refers to a mole of gas before entering the shock wave.

METHODS OF CALCULATION

Excitation Calculations

When there is no electronic excitation or ionization in a monatomic gas, the flow properties before and after a normal shock wave can be given by the equations of continuity, momentum, and energy and the perfect gas laws. These are as follows:

continuity

$$u_1 V_2 = u_2 V_1 \tag{1}$$

momentum

$$p_1 + \frac{u_1^2}{V_1} = p_2 + \frac{u_2^2}{V_2} \tag{2}$$

energy

$$E_1 + p_1 V_1 + \frac{1}{2} u_1^2 = E_2 + p_2 V_2 + \frac{1}{2} u_2^2 \tag{3}$$

state

$$p_1 V_1 = RT_1 \tag{4}$$

$$p_2 V_2 = RT_2 \tag{5}$$

where the internal energies E_1 and E_2 are given by $\frac{3}{2} RT_1$ and $\frac{3}{2} RT_2$, respectively. If a shock-flow problem is adequately specified, these five equations uniquely determine the unknown flow properties.

For a real monatomic gas, the temperatures encountered in strong shock waves induce electronic excitation and ionization which become important and make the equation of state (5) and the expression for E_2 no longer valid. The correction for ionization and electronic excitation is made in the following manner: First, the equation of state which is true for a constant number of moles of particles per unit mass of gas is changed to

$$p_2 V_2 = \left(1 + \frac{\alpha}{100}\right) RT_2 \tag{6}$$

so as to include the increased number of particles due to ionization, where α is the percent ionization in a shock wave when there is no ionization of the gas entering the shock. Second, the energy E_2, which is no longer given by $\frac{3}{2}RT_2$, is the sum of the energies of translation, ionization, and excitation; that is,

$$E_2 = E_t + E_{ion} + E_{ex} \tag{7}$$

where

$$E_t = \frac{3}{2} R \left(1 + \frac{\alpha}{100}\right) T_2 \tag{8}$$

$$E_{ion} = \frac{\alpha}{100} N_o \chi\sigma \tag{9}$$

$$E_{ex} = RT_2^2 \left[\left(1 - \frac{\alpha}{100}\right) \frac{d}{dT} \left(\log Z_{I_i}\right) + \frac{\alpha}{100} \frac{d}{dT} \left(\log Z_{II_i}\right) \right]_{T=T_2} \tag{10}$$

The energy expressions (eqs. (8) to (10)) are given in section II of reference 1 for a diatomic gas. They are altered here to apply to a monatomic gas by dropping terms corresponding to molecular vibration, rotation, and dissociation.

The value of α is determined from the equilibrium constant K which is related by Saha's equation to the partition functions and the temperature of the gas (ref. 1). Thus,

$$\frac{\left(\frac{\alpha}{100}\right)^2}{1 - \frac{\alpha}{100}} = K = \frac{Z_{II} Z_e}{Z_I N_o} e^{-\chi\sigma/kT_2} \tag{11}$$

from which there is obtained

$$\alpha = \frac{-K + \sqrt{K^2 + 4K}}{2} 100 \tag{12}$$

In this analysis, the temperatures considered are not high enough for double ionization of an appreciable number of atoms. The number of doubly ionized atoms is therefore neglected, and α represents the percent of atoms that are singly ionized.

The partition functions of the atoms Z which appear in equations (10) and (11) are defined by

$$Z_I = Z_{I_t} Z_{I_i} \tag{13}$$

where

$$Z_{I_t} = \frac{\left(2\pi m_I kT_2\right)^{3/2}}{h^3} V_2 \tag{14}$$

$$Z_{I_i} = \sum_{n=0}^{\infty} g_{I_n} e^{-\tilde{\nu}_{I_n} hc/kT_2} \tag{15}$$

and

$$Z_{II} = Z_{II_t} Z_{II_i} \tag{16}$$

where

$$Z_{II_t} = \frac{\left(2\pi m_{II} kT_2\right)^{3/2}}{h^3} V_2 \tag{17}$$

$$Z_{II_i} = \sum_{n=0}^{\infty} g_{II_n} e^{-\tilde{\nu}_{II_n} hc/kT_2} \tag{18}$$

For an electron,

$$Z_e = Z_{e_t} Z_{e_i} \tag{19}$$

where

$$Z_{e_t} = \frac{(2\pi m_e k T_2)^{3/2}}{h^3} V_2 \tag{20}$$

$$Z_{e_i} = 2 \tag{21}$$

These equations are standard expressions of statistical mechanics and equivalent forms may be found, for example, in reference 1. They are based on the assumption of thermal equilibrium. The summations indicated by equations (15) and (18) extend over all the electronic energy levels of each atom type, that is, the neutral and the ionized atoms. The term-value differences measured from the ground states are $\tilde{\nu}_{I_n}$ and $\tilde{\nu}_{II_n}$ and the g's are the statistical weights. For the nth state, g_n is $2J_n + 1$ where J is the total angular-momentum quantum number as given in reference 6.

With these revisions, ionization and excitation effects are included in the analysis. The equations to be solved are equations (1) to (4), (6), and (11) and the relations for E_2 given by equations (8) to (21). The procedure for the calculations is as follows.

By using spectroscopically determined term-value differences for each atom type, Xe_I and Xe_{II}, up to $\tilde{\nu}_{I_n} = 97{,}007.41\ cm^{-1}$ and $\tilde{\nu}_{II_n} = 157{,}225.10\ cm^{-1}$, respectively (see ref. 6), the internal part of the partition functions (eqs. (15) and (18)) are calculated for values of T_2 ranging from 300° K to 3,000° K in intervals of approximately 500° K. The variation of these partition functions with temperature is shown in figure 1. From these curves the two $RT_2^2 \frac{d}{dT} \log Z_i$ terms in equation (10) are determined and are plotted as a function of T_2 (see fig. 2).

The total partition functions from equations (13), (16), and (19) are then determined for various values of T_2 and are substituted into equation (11) to obtain α as a function of T_2 and V_2. The ionization α is then plotted as a function of T_2. For a given value of V_2, the corresponding values of α, $RT_2^2 \frac{d}{dT} \log Z_{I_i}$, and $RT_2^2 \frac{d}{dT} \log Z_{II_i}$ are substituted into equations (8) to (10), and the energy E_2 is plotted as a function of T_2.

In order to satisfy a shock-flow condition, the proper value of E_2 is determined by use of equations (1) to (3) which relate conditions before and after the shock. If u_1, u_2, and p_2 are eliminated from equations (1) to (4) and (6), then

$$E_2 = \frac{1}{2} RT_1 \left\{ \left[1 + \left(1 + \frac{\alpha}{100} \right) \frac{T_2}{T_1} \frac{V_1}{V_2} \right] \left(1 - \frac{V_2}{V_1} \right) + 3 \right\} \tag{22}$$

Standard conditions are chosen for p_1, V_1, and T_1. Since α is known as a function of T_2 and V_2, this second expression for E_2 is plotted as a function of T_2 for the given value of V_2. The two functions of E_2 are compared on the same graph for the same value of V_2. They form two intersecting curves which fix the values of E_2 and T_2 for one shock condition. From these values the unknown flow conditions u_1, u_2, and p_2 are determined. Different shock conditions are calculated by selecting a different value of V_2 and by following the same procedure. The final results are plotted as a function of Mach number of the undisturbed stream.

Nonexcitation Calculations

Resler, Lin, and Kantrowitz (ref. 4) have shown that electronic excitation can be neglected for flows in argon up to $M_1 = 20$. Since the electronic excitation levels of xenon differ from those of argon, calculations are made to show the results when the electronic excitation of xenon is neglected. The equations used are equations (1) to (4), (6), and

$$E_2 = E_t + E_{ion} = \frac{3}{2} R\left(1 + \frac{\alpha}{100}\right)T_2 + \frac{\alpha}{100} N_o \chi\sigma \tag{23}$$

to which equation (7) reduces when excitation is neglected. In this case the internal part of the partition functions for the atoms in equations (15) and (18) reduces to the first term of the summation series. Thus, equations (13) and (16) become

$$Z_I = \frac{(2\pi m_I k T_2)^{3/2}}{h^3} g_{I_o} V_2 \tag{24}$$

and

$$Z_{II} = \frac{(2\pi m_{II} k T_2)^{3/2}}{h^3} g_{II_o} V_2 \tag{25}$$

where

$$g_{I_o} = 1$$

and

$$g_{II_o} = 4$$

as obtained from reference 6.

Using this result gives Saha's equation in the following form:

$$K = 8\left(\frac{2\pi m_e k}{h^2}\right)^{3/2} \frac{V_2 T_2^{3/2}}{N_o} e^{-\chi\sigma/kT_2} \tag{26}$$

where the mass ratio m_{II}/m_I is approximated as unity.

In order to determine the flow conditions of a shock wave by this method, the percent ionization from equation (12) is plotted as a function of T_2 for a given value of V_2 and the energy E_2 in equation (23) is then plotted as a function of T_2. As in the preceding case, values

of E_2 and T_2 which satisfy equations (22) and (23) for the given value of V_2 are determined graphically. All the properties of the flow are then determined as functions of the free-stream Mach number.

RESULTS OF CALCULATIONS

The excitation calculations and the nonexcitation calculations are made for one-dimensional shock waves in xenon up to $M_1 = 15$. Standard conditions are assumed in the undisturbed flow which are $p_1 = 1{,}013{,}250$ dynes/cm^2, $T_1 = 273.16^\circ$ K, and $V_1 = 22{,}420.8$ cm^3/mole. The values of constants used in the calculations are obtained from references 7 and 8. The results of the calculations, together with the appropriate ideal-flow quantities, are presented in graphical form plotted against Mach number of the undisturbed flow. Percent ionization, temperature, specific-volume ratio, pressure ratio, and stream velocity behind the shock wave are shown in figures 3, 4, 5, 6, and 7, respectively.

Generally it is evident that the noticeable effects of ionization and excitation begin at approximately $M_1 = 8$ and increase as the speed of the shock increases (fig. 3). When ionization and excitation are present, these processes absorb part of the energy of the gas and leave less translational energy than for the ideal flow. As an almost direct result, the excitation-calculation temperature is less than the ideal-flow temperature (fig. 4). The specific-volume ratio and the pressure ratio are influenced by two effects, namely, the lowered temperature and the change in the number of particles per unit mass of gas (a direct result of ionization). In addition, of course, they are related to each other by the equation of state. The net result is that the excitation-calculation specific-volume ratio is considerably greater than in the ideal-flow case (fig. 5) and that the excitation-calculation pressure ratio is somewhat larger than in the ideal-flow case (fig. 6). The excitation-calculation stream velocity behind the shock reaches a maximum at $M_1 \approx 12$, whereas in the ideal-flow case it continues to increase (fig. 7).

A comparison of the results of the excitation calculation and the nonexcitation calculation shows that, within the range of the present calculations, the effect of excitation is of the order of 10 percent of the effect of ionization. When the assumption is made that no energy of the gas is absorbed as excitation energy, more energy is available for ionization and translation. Thus, the nonexcitation percent ionization is larger than the excitation percent ionization (fig. 3) and the nonexcitation temperature is larger than the excitation temperature (fig. 4).

The results of the two methods of calculation for specific-volume ratio, pressure ratio, and stream velocity after the shock are in agreement with the physically plausible concept that calculations in which excitation effects are neglected should give results that are less different from the ideal-flow case than calculations in which excitation effects are included. The differences between these two calculations increase as the flow speed increases.

Figure 8 shows the turning angle of the stream through two types of shock waves which have various inclinations. The excitation-calculation results are compared with those of the ideal-flow case. Since the presence of excitation and ionization causes the stream velocity to be smaller after the shock, the stream turning angle is greater in this case. Larger turning angles in this flow indicate that at a given Mach number the same angle of shock is obtained by a blunter shaped body. The values of shock inclinations about conical-shaped bodies in an axisymmetrical ideal flow are given in table I. The shock angles are calculated for a monatomic gas where $\gamma = 5/3$ by the method described in reference 9.

The effects of electronic excitation can be neglected for flows in some gases. Resler, Lin, and Kantrowitz (ref. 4) showed that this situation is true for the case of argon since for flow velocities as high as $M_1 = 20$ the amount of electronic excitation energy is approximately 1.7 percent of the total internal energy of the gas. For a flow in xenon this proportion of electronic excitation energy is present in the shock wave at $M_1 = 11.2$ (see fig. 9) and becomes 13.3 percent at $M_1 = 15$. Thus, the effect of electronic excitation is much more important in xenon than in argon.

COMPARISON OF THEORETICAL AND EXPERIMENTAL RESULTS

If the presence of ionization in a shock wave is assumed to be characterized by a glowing phenomenon and the intensity of the glow is assumed to be approximately proportional to the percent of ionization, a qualitative comparison can be made between the results of reference 3 and theory. For this purpose figures 8 to 10 of reference 3 which show flows in xenon about cone-cylinder models are reproduced as figures 10 to 12. In addition, the flow about a small steel sphere is shown in figure 13. Figure 13 was obtained by the apparatus used in reference 3. The test results are given in table II.

The calculations show that ionization is present in a shock wave for Mach numbers greater than approximately 8. Figures 10 to 12 indicate this occurrence to be approximately true for the actual shock flows. A glow is seen in the shock wave of figure 10 where the Mach number normal to this shock M_1 is 9.0 and this glow covers the silhouette of the

cone part of the cone-cylinder model. For this case, theory indicates 0.06 percent ionization (see table II). When the Mach number normal to the shock is reduced, the intensity of the glow in the shock wave diminishes nearly proportionally until it is no longer visible. Figures 11 and 12 show cases of strong shock flows where the intensity of the glow is not observed. In figure 11, the Mach number normal to the shock wave is 4.9. The theory indicates no appreciable ionization in a shock wave of this strength. Likewise, figure 11 shows that there is no glow on the silhouette of the cone part of the cone-cylinder model to correspond to that in figure 10. The flow about the cone-cylinder model in figure 12 indicates the approximate Mach number range in which glow begins. The model is yawed 4° to the free-stream direction. The normal Mach number of the shock about this yawed cone varies from 8 to 10. A glow is associated with the greatest shock inclination and no glow is associated with the least shock inclination; this result corresponds to theory. As would be expected from theory, figure 13 shows a more intense glow than figure 10 since 2.9-percent ionization is calculated for the sphere compared to 0.06 percent for the cone-cylinder model.

CONCLUDING REMARKS

The work of Resler, Lin, and Kantrowitz indicates that simplified calculations may be used to determine the flow properties of strong shock waves in argon because the electronic excitation energy is small compared to the total internal energy. These investigators use these simplified calculations for flow velocities up to a Mach number normal to shock M_1 of 20 without large error. In the present investigation it is found by comparison with more exact calculations that the effect of electronic excitation is much more important for xenon than argon. The difference between excitation and nonexcitation calculations increases with increases in flow speed.

The flow properties which are calculated by considering the effects of electronic excitation and ionization are compared with ideal-flow properties. Differences occur between these two flows when ionization is present. The differences increase as the ionization increases at larger flow speeds. The calculations show that the actual temperature and stream velocity behind the shock wave are less than in the ideal case, whereas the pressure ratio and specific-volume ratio across the shock are greater. The real stream velocity behind the shock reaches a maximum value as the speed increases and then decreases.

The results of the calculations are qualitatively compared with available experimental results. At shock speeds above approximately $M_1 = 8$ the experimental results show a visible glow in the shock.

If the assumption that the intensity of the glow is approximately proportional to the percent of ionization is used, the experimental results appear to be in qualitative agreement with the results of calculations.

Langley Aeronautical Laboratory,
National Advisory Committee for Aeronautics,
Langley Field, Va., September 25, 1953.

REFERENCES

1. Doering, W., and Burkhardt, G.: Contributions to the Theory of Detonation. Tech. Rep. No. F-TS-1227-IA, Air Materiel Command, U. S. Air Force, May 1949.

2. Bethe, H. A., and Teller, E.: Derivations From Thermal Equilibrium in Shock Waves. Rep. No. X-117, Ballistic Res. Lab., Aberdeen Proving Ground, 1945.

3. Donaldson, Coleman duP., and Sabol, Alexander P.: Experiments on Aerodynamic Phenomena at Mach Numbers in the Range From 10 to 20. Proc. First U. S. Nat. Cong. Appl. Mech. (Chicago, Ill., 1951), A.S.M.E., 1952, pp. 757-762.

4. Resler, E. L., Lin, Shao-Chi, and Kantrowitz, Arthur: The Production of High Temperature Gases in Shock Tubes. Jour. Appl. Phys., vol. 23, no. 12, Dec. 1952, pp. 1390-1399.

5. Eckerman, J., and Schwartz, R. N.: Observations on the Luminescence Accompanying Cone-Cylindrical and Spherical Missiles Traveling at High Speeds. Phys. Rev. (Abstract in Proceedings of the American Physical Society), vol. 87, no. 5, Second ser., Sept. 1, 1952, p. 912.

6. Thon, N., ed.: Annual Tables of Physical Constants. Frick Chemical Lab. (Princeton, N. J.), 1942.

7. DuMond, Jesse W. M., and Cohen, E. Richard: Recent Advances in Our Knowledge of the Numerical Values of the Fundamental Atomic Constants. American Scientist, vol. 40, no. 3, July 1952, pp. 447-467.

8. Hodgman, Charles D., ed.: Handbook of Chemistry and Physics. Thirtieth ed., Chemical Rubber Publishing Co., 1947, p. 2631.

9. Ferri, Antonio: Elements of Aerodynamics of Supersonic Flows. The Macmillan Co., 1949, pp. 236-260.

TABLE I

PROPERTIES OF SYMMETRICAL CONICAL SHOCK FLOW IN AN IDEAL GAS

$[\gamma = 5/3]$

δ, deg	u_c/u_l	M	θ	δ, deg	u_c/u_l	M	θ
5	0.650	1.5283	40° 58'	30	0.400	1.5700	66° 8'
	.800	2.4048	24° 46'		.600	2.3327	46° 6'
	.860	3.1900	19° 19'		.650	2.8481	43°
	.870	3.2202	18° 25'		.700	3.5369	41° 1'
	.880	3.3898	17° 32'		.750	4.5525	38° 3'
	.950	5.8263	10° 56'		.785	6.4434	36° 38'
	.970	8.0133	8° 52'		.800	8.3343	36° 4'
	.975	9.7652	8° 16'		.810	11.1318	35° 42'
	.980	10.5961	7° 41'		.814	13.0189	35° 34'
	.990	18.5376	6° 27'		.815	13.7233	35° 31'
					.818	17.6227	35° 26'
10	.700	1.9498	33° 9'		.820	21.5499	35° 20'
	.800	2.6190	24° 30'				
	.850	3.2402	20° 43'	40	.400	2.3018	65° 44'
	.875	3.6968	18° 55'		.500	2.8061	57° 31'
	.922	5.2171	15° 38'		.600	4.3203	51° 41'
	.950	7.4371	13° 41'		.632	5.6989	50° 11'
	.970	12.8992	12° 16'		.650	7.2907	49° 25'
	.972	14.4189	12° 8'		.667	11.2260	48° 43'
	.974	16.4326	11° 59'		.675	17.6869	48° 23'
	.976	19.8942	11° 50'		.676	20.3139	48° 20'
20	.600	1.7521	42° 58'	45	.375	3.1767	68° 56'
	.700	2.3300	34° 53'		.400	3.2403	66° 52'
	.800	3.4521	28° 52'		.500	4.5126	59° 55'
	.825	3.9399	27° 37'		.525	5.3483	58° 32'
	.850	4.6710	26° 23'		.535	5.9554	57° 59'
	.860	5.0613	25° 56'		.550	7.1028	57° 14'
	.870	5.5861	25° 26'		.570	11.7769	56° 19'
	.880	6.2865	25° 3'		.575	14.4478	56° 3'
	.890	7.2219	24° 34'		.578	18.4953	55° 55'
	.900	8.7875	24° 6'		.580	22.4356	55° 49'
	.910	12.7897	23° 52'				
	.916	16.8710	23° 26'				
	.920	28.1718	23° 15'				

TABLE II

EXPERIMENTAL TEST RESULTS OF SMALL CONE-CYLINDER MODELS AND SPHERES FIRED INTO XENON GAS

Figure	δ, deg	Model velocity, cm/sec	T_1, $^\circ K$	Free-stream Mach number, M	θ, deg (observed)	α, percent (calculated)
[a]10	45.0	194,923	296.4	11.0	56° 31.0'	0.06
[a]11	22.5	192,116	297.6	10.8	26° 45.5'	0
[a]12	45.0	183,446	295.8	10.4	---------	----
13	90.0	219,456	294.1	12.5	---------	2.9

[a]Data obtained from reference 3.

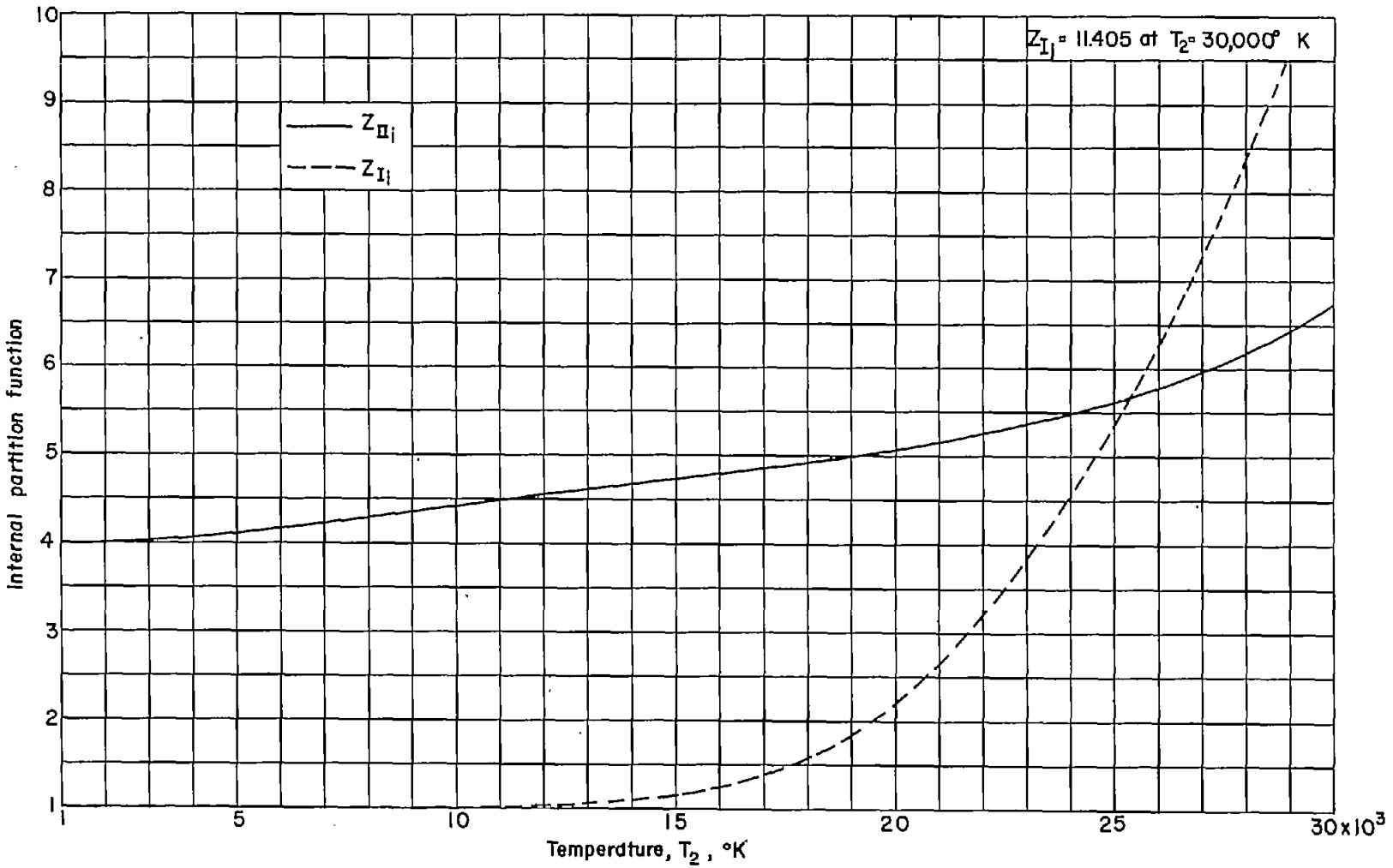

Figure 1.- Variation of internal partition functions Z_{II_i} and Z_{I_i} with temperature.

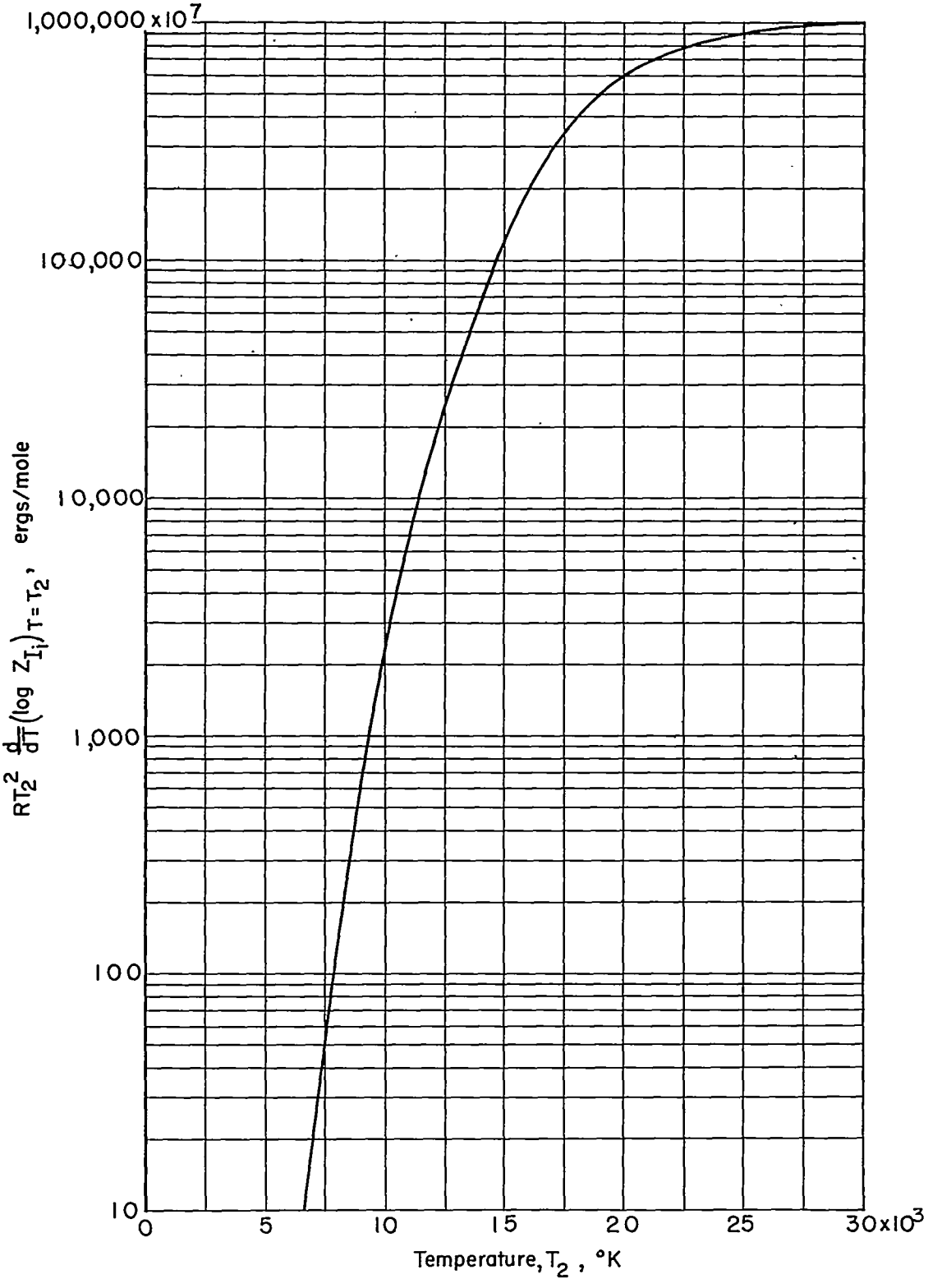

Figure 2.- Variation of electronic excitation energy with temperature.

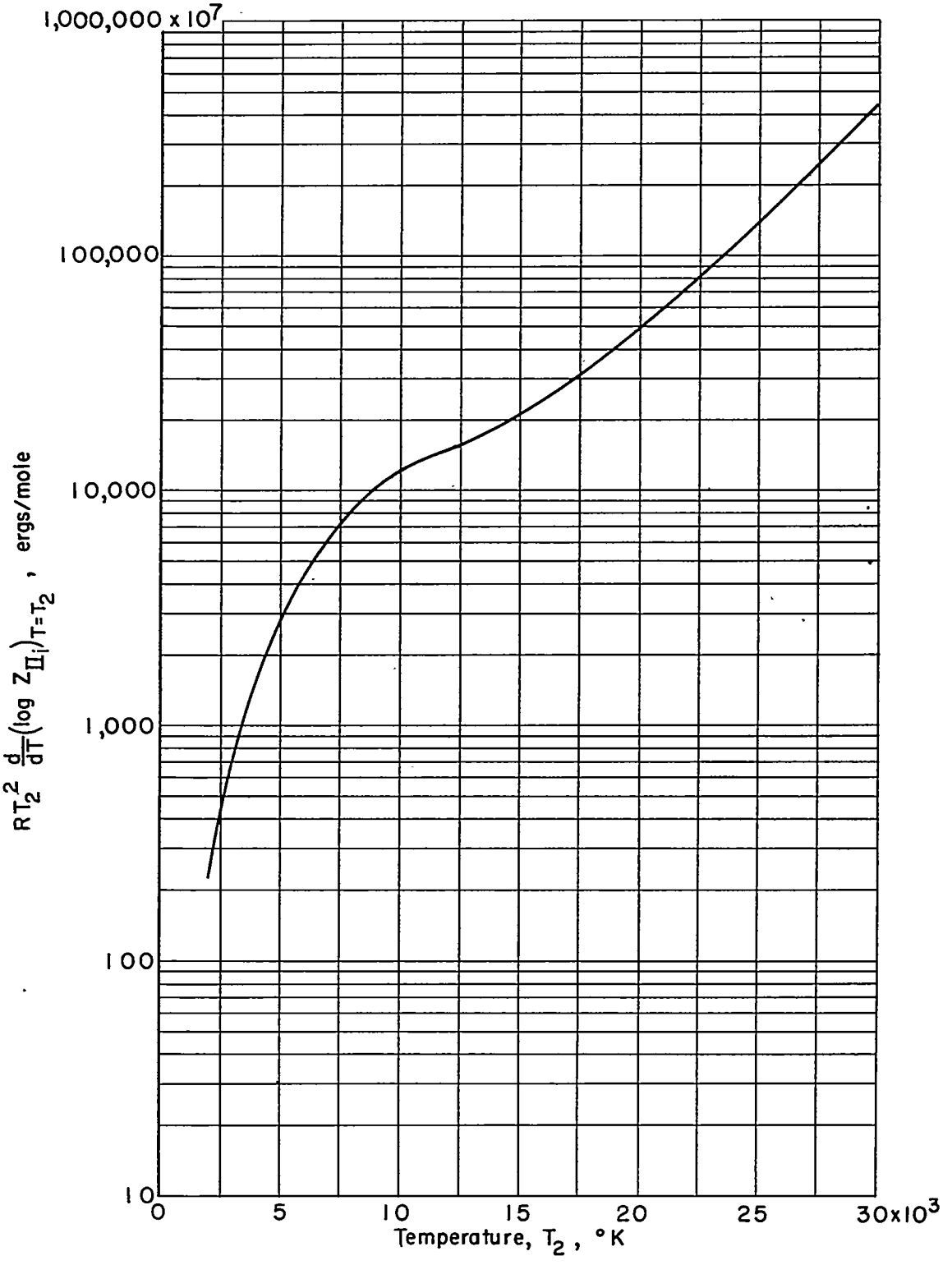

Figure 2.- Concluded.

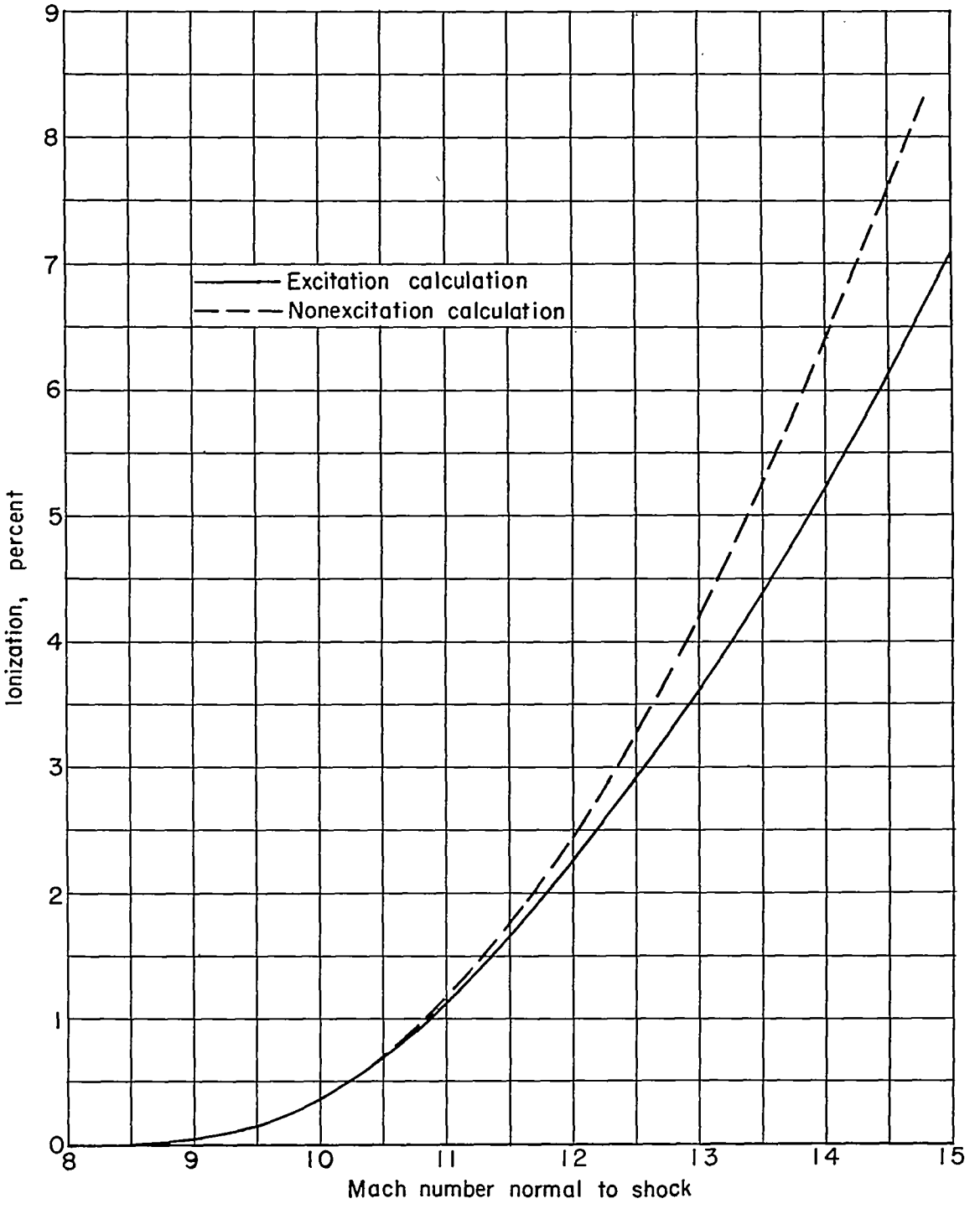

Figure 3.- Percent ionization calculated for shock waves in xenon.

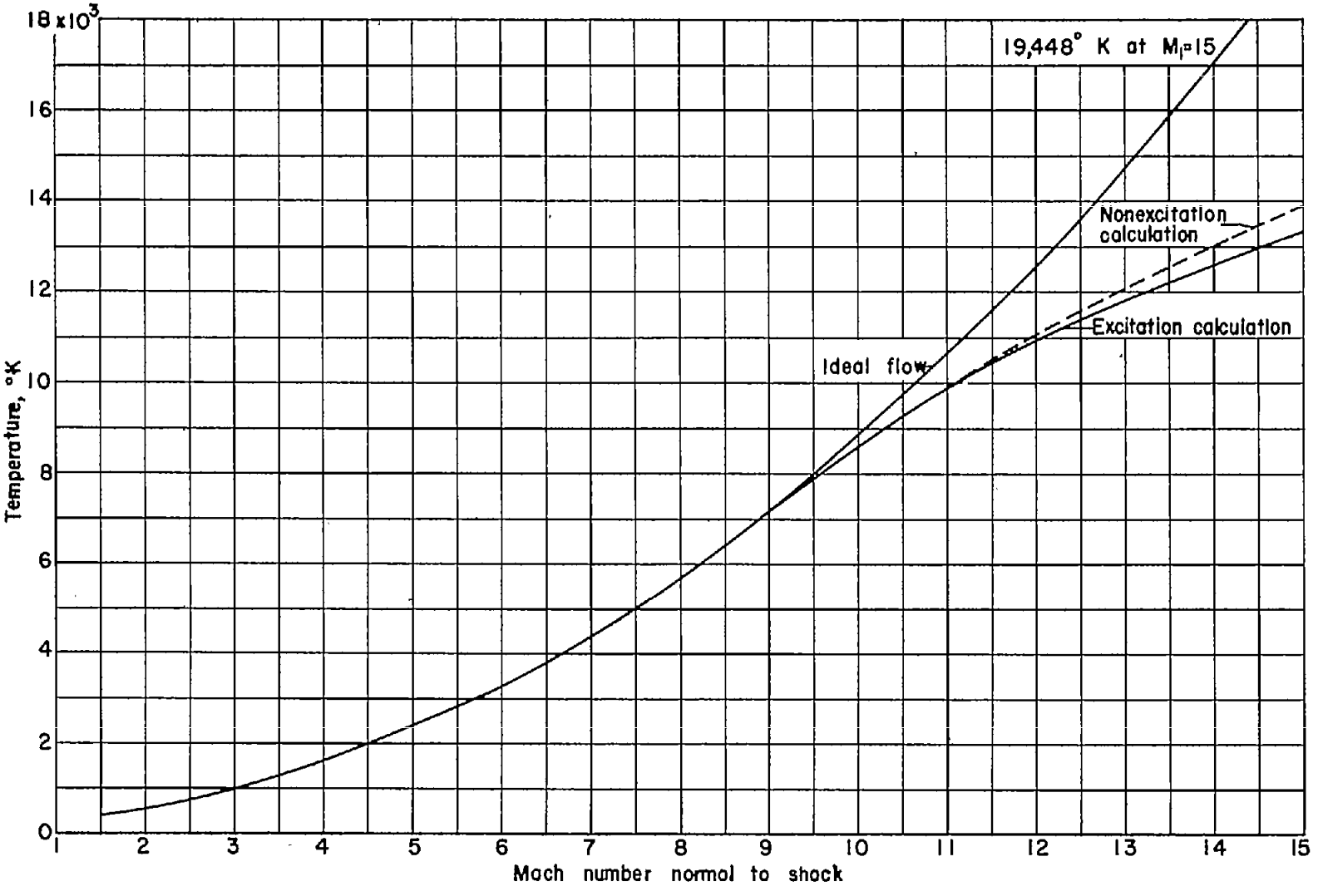

Figure 4.- Variation of temperature in shock wave with Mach number normal to shock.

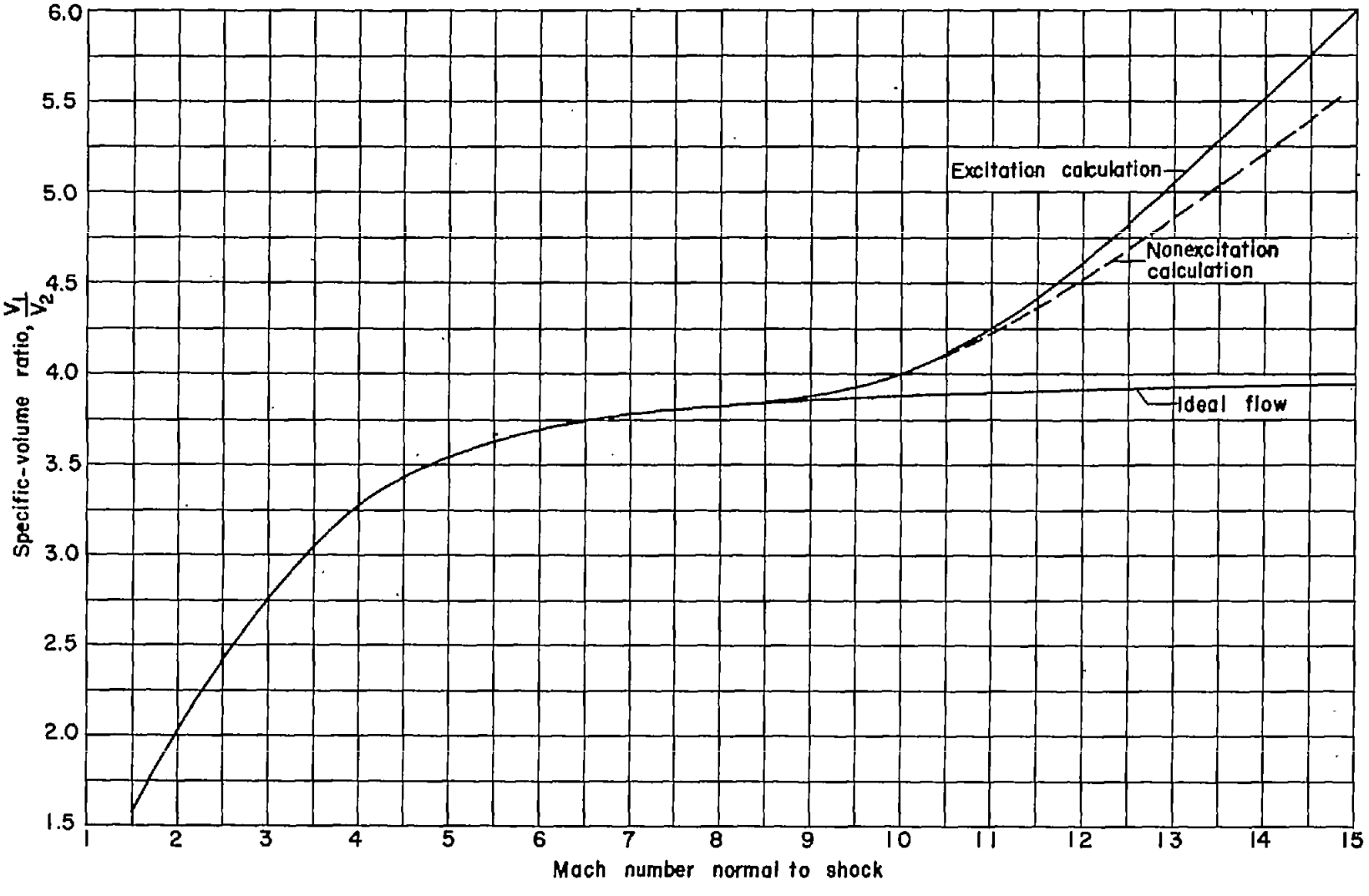

Figure 5.- Variation of specific-volume ratio with Mach number normal to shock.

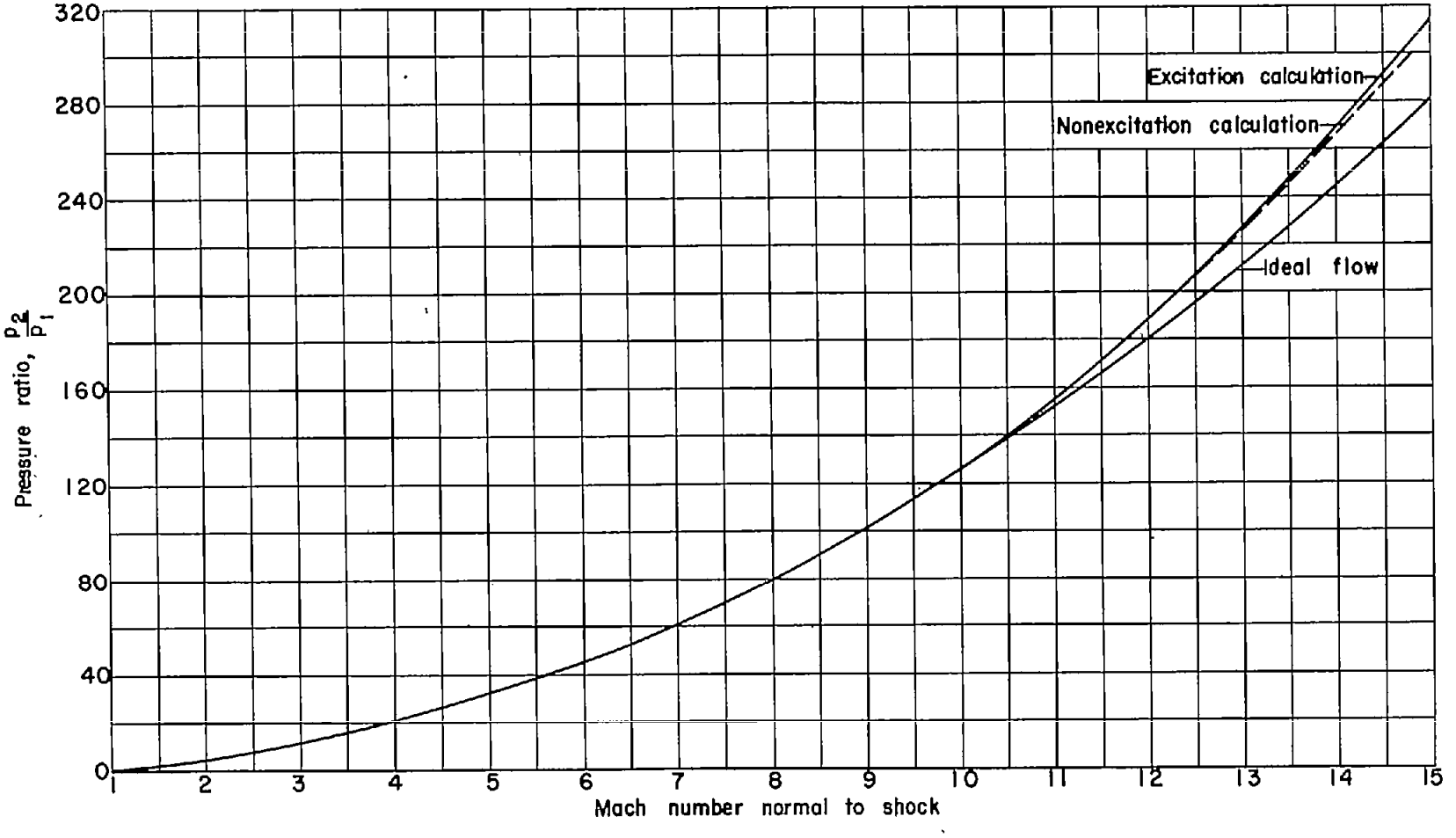

Figure 6.- Variation of pressure ratio with Mach number normal to shock.

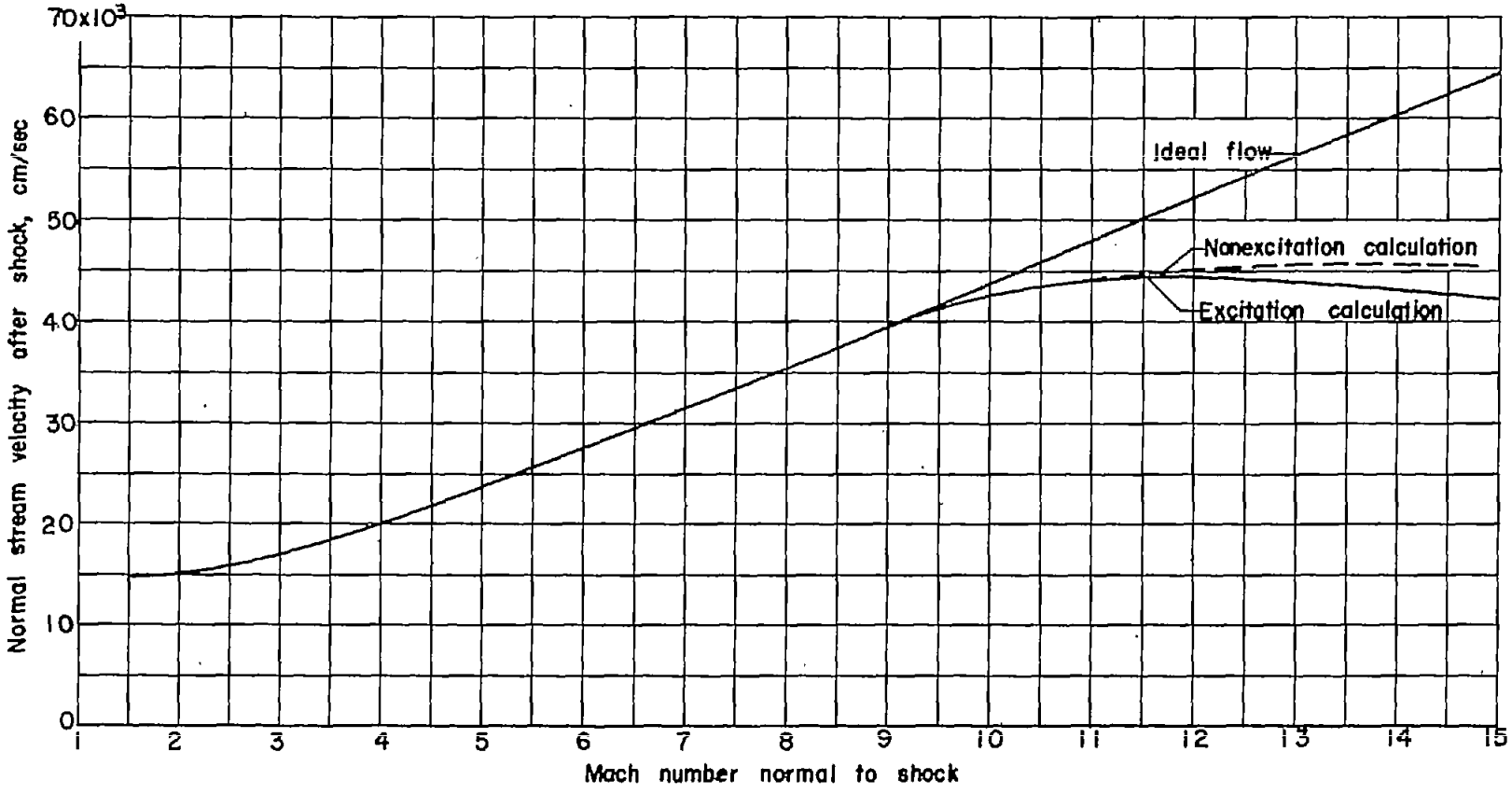

Figure 7.- Variation of normal stream velocity after shock with Mach number normal to shock.

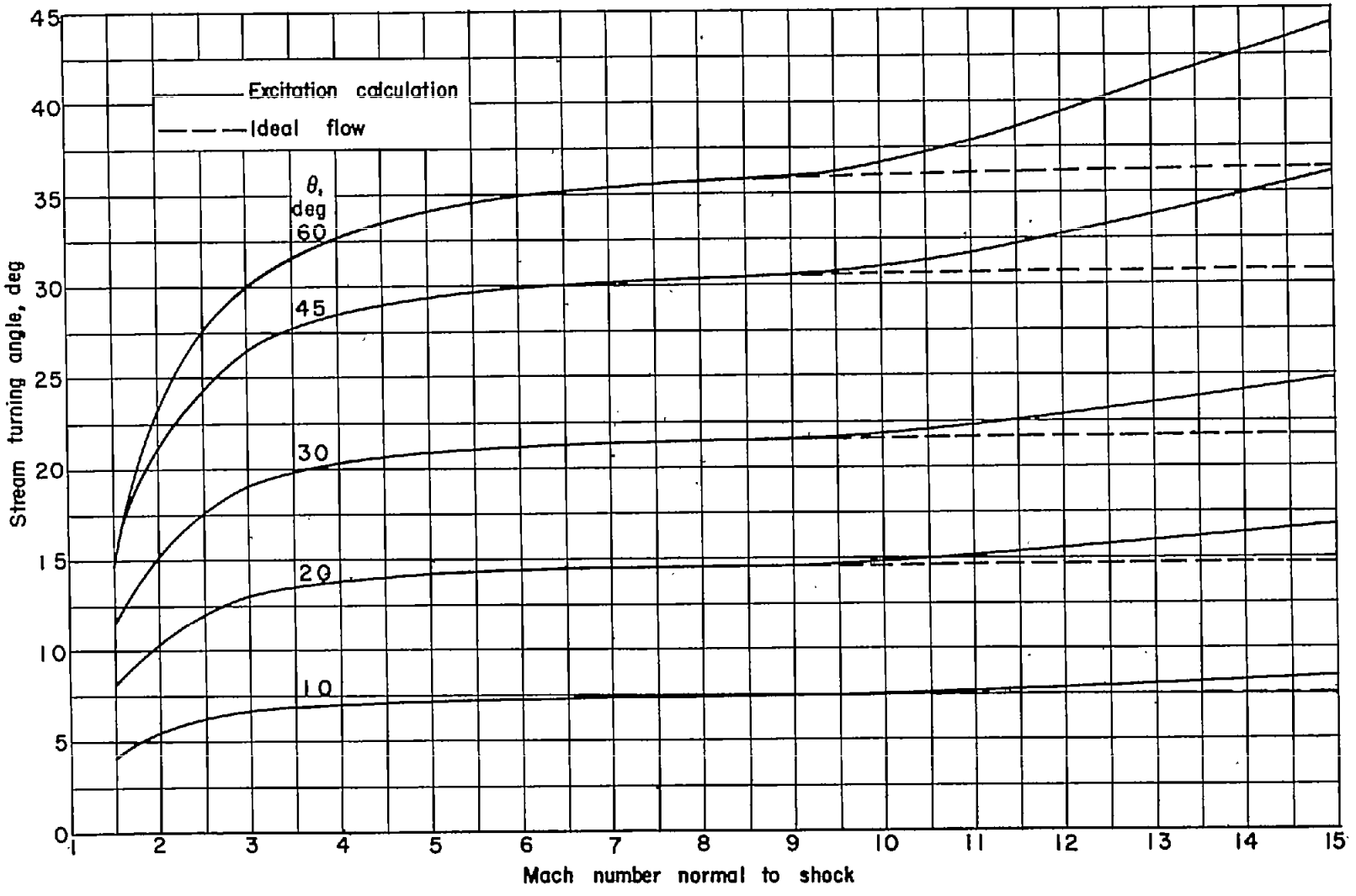

Figure 8.- Stream turning angle through a shock wave with and without ionization.

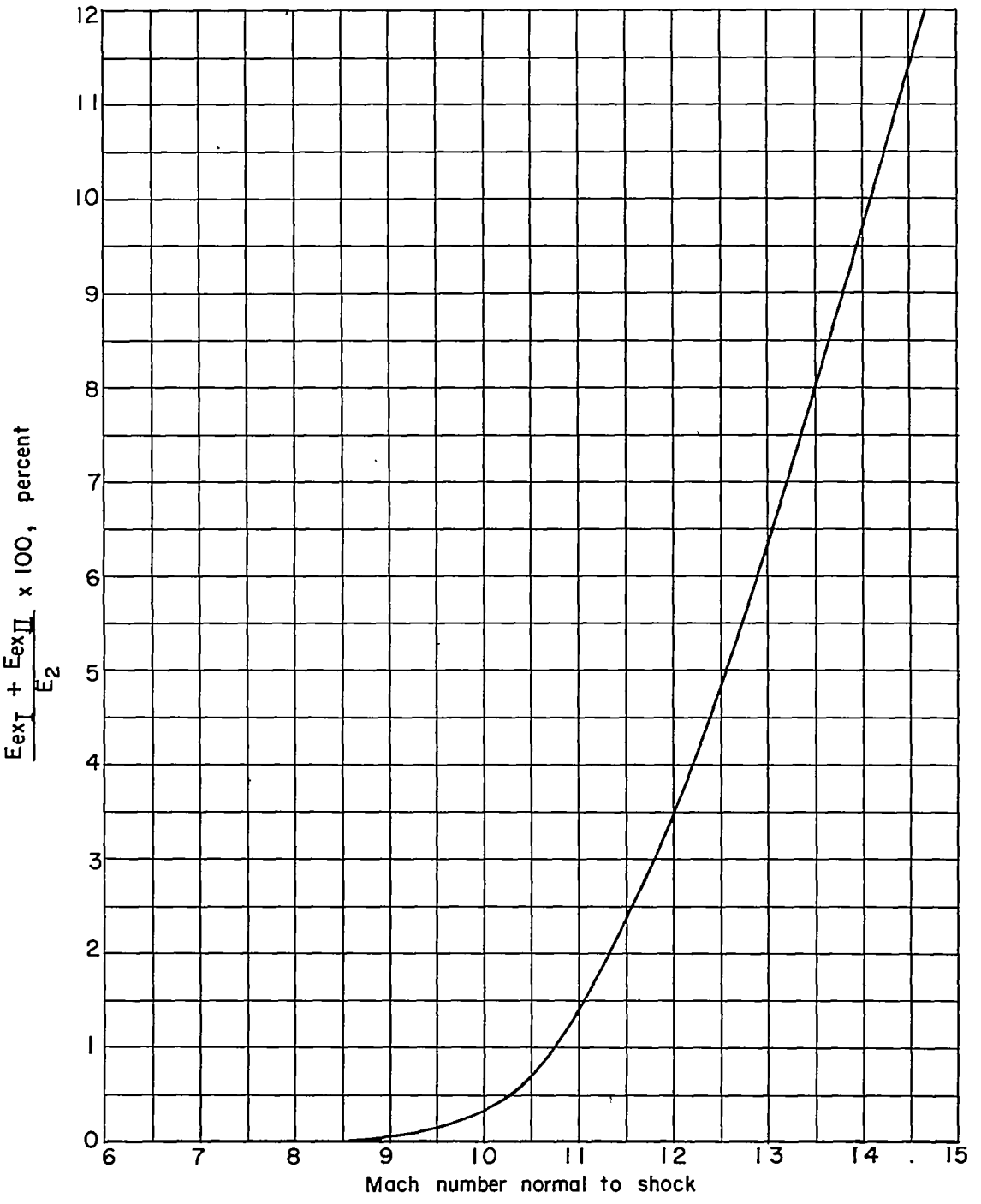

Figure 9.- Percent of excitation energy in a shock wave.

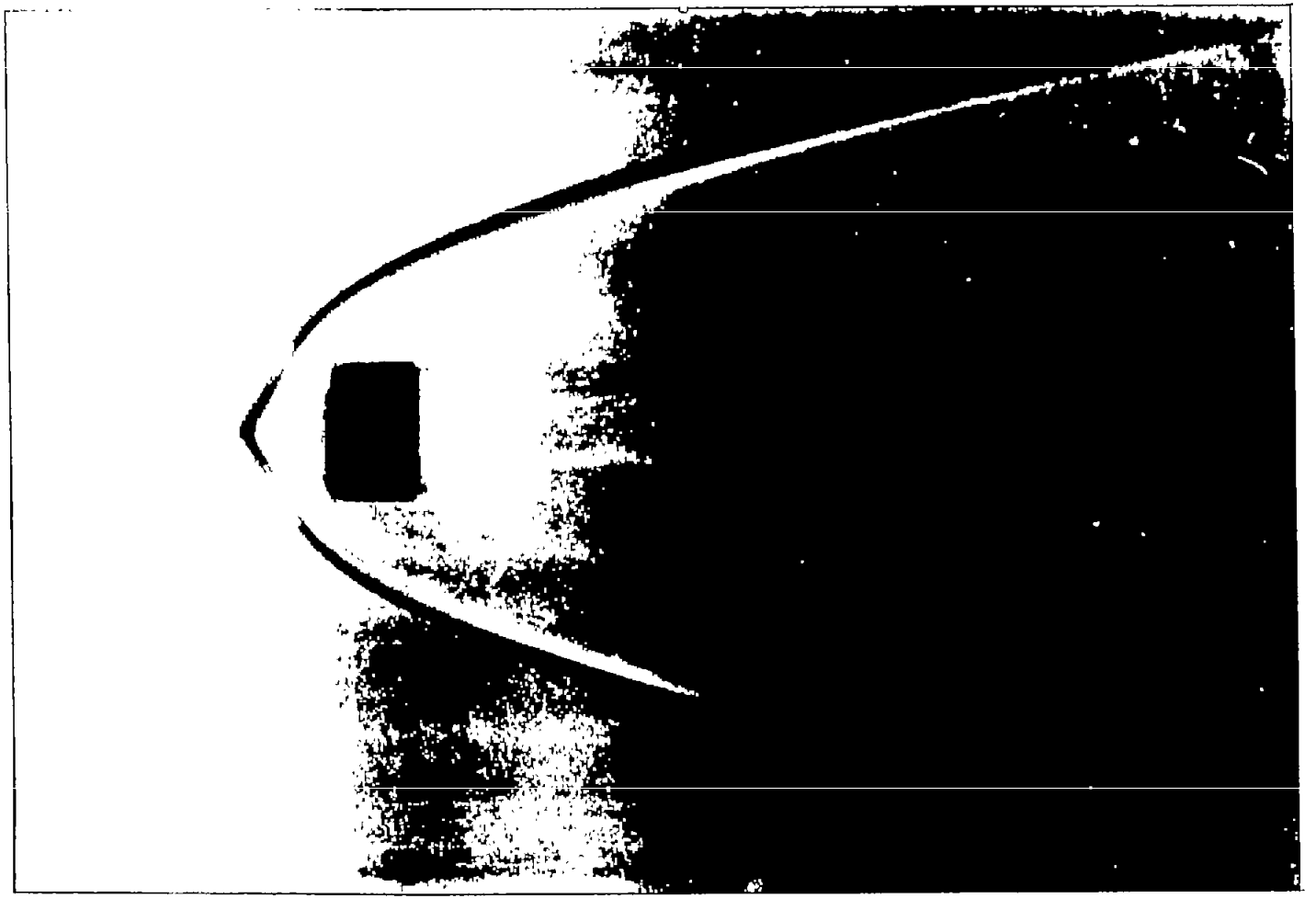

L-81272

Figure 10.- A shadowgraph of the flow phenomenon about a 90° cone-cylinder model traveling at M = 11.0.

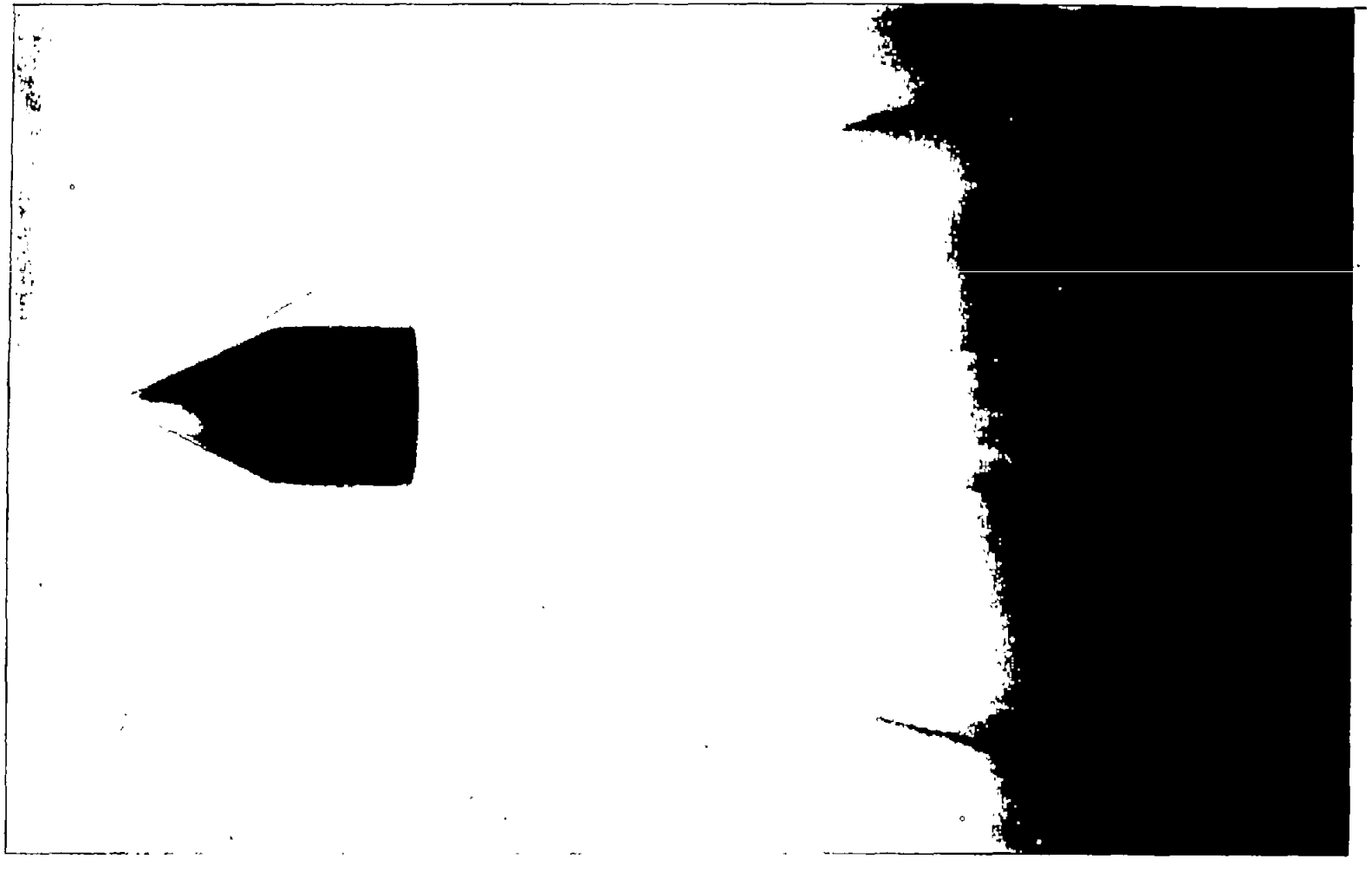

L-81273

Figure 11.- A schlieren photograph of the flow phenomenon about a 45° cone-cylinder model traveling at M = 10.8.

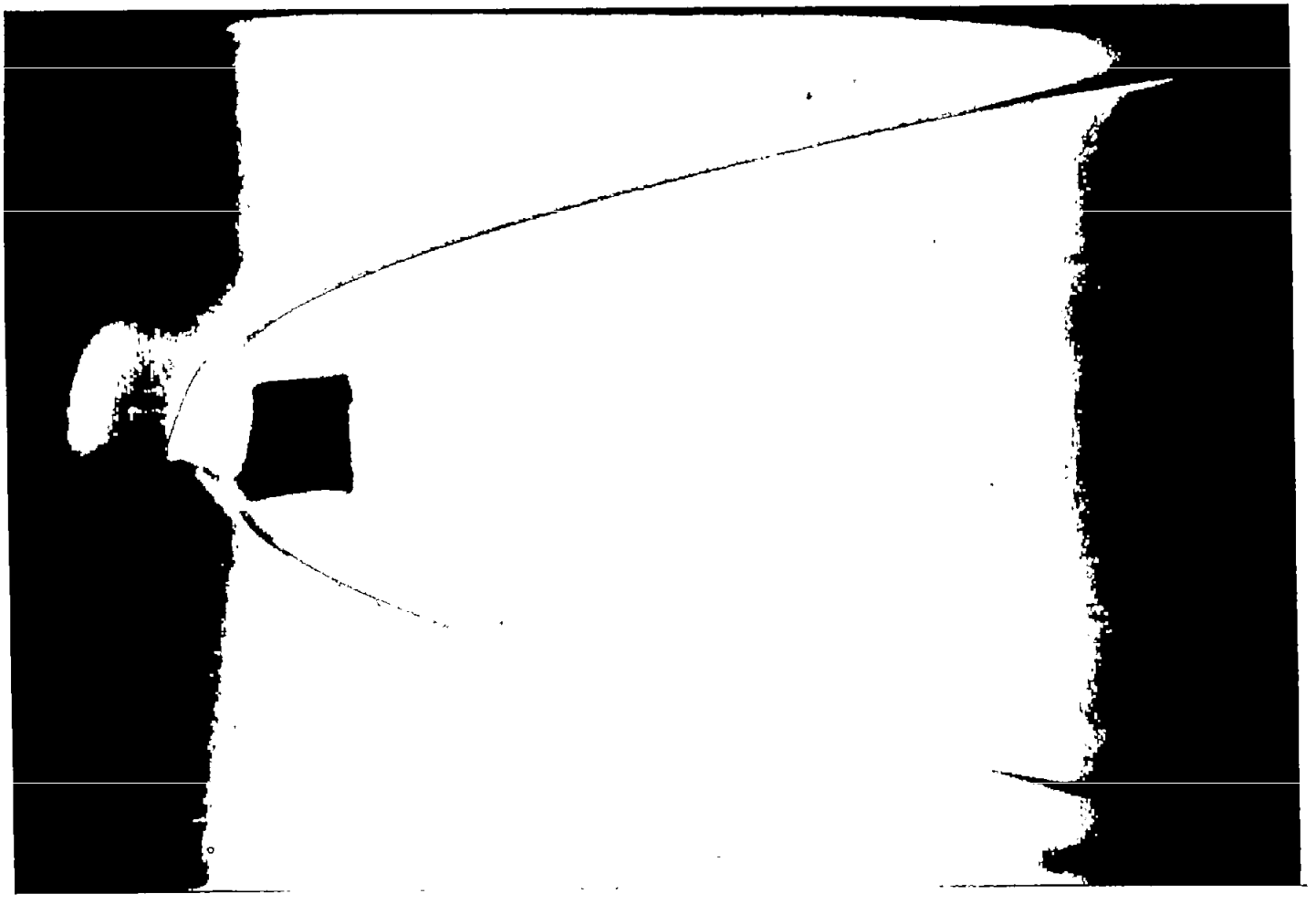

L-81274

Figure 12.- A shadowgraph of the phenomenon about a yawed 90° cone-cylinder model traveling at M = 10.4. Angle of yaw, 4°.

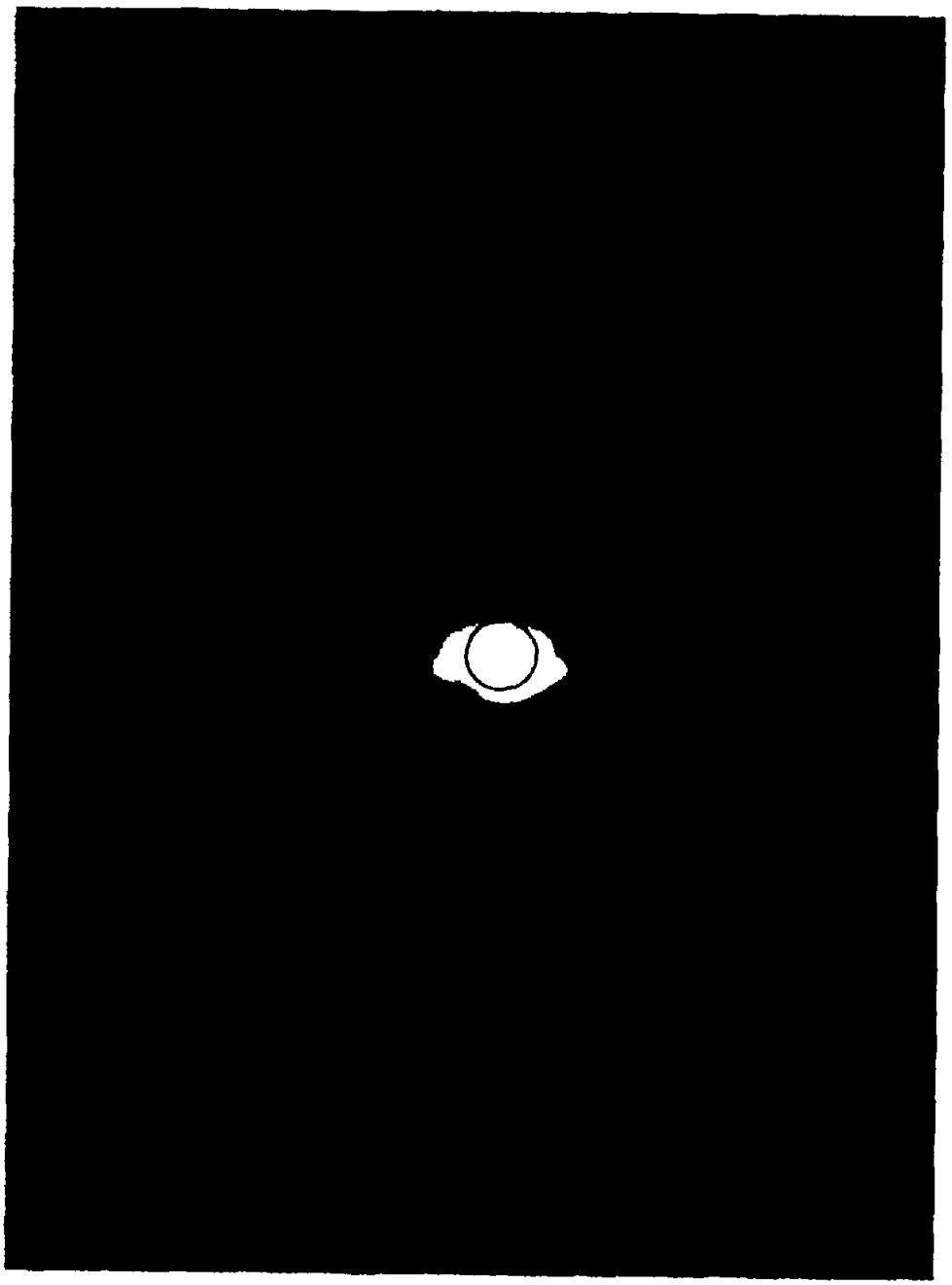

L-80264

Figure 13.- Photograph of the glowing area about a steel sphere traveling at M = 12.5. Approximate contour of model is added to the photograph.

NACA-Langley - 12-23-53 - 1000